Acta Technica *62* (2017), No. 6A, 273–282

Research on efficient wireless power transmission system for EV

Zhao Zhenyu[1], Guo Weishang[1], Song Xueying[1 2]

Abstract. Because of the LCL-S wireless power transmission (WPT) system has the characteristics of constant primary current and secondry voltage; it has been widely used in the field of small power electric vehicle charging system. However, when the system is light loaded, the output current of the inverter is distorted, which is the inherent shortcoming of the LCL-S WPT system. To solve this problem, the modified methods is proposed on the basis of not affecting the original characteristics of the electric vehicle wireless charging system. The working principle of the improved methods and the rewarding results can be obtained theoretically. Finally, simulation analysis and experimental results can prove the correctness of the theoretical analysis.

Key words. LCL-S; wireless power transmission; distortion; improvement.

1. Introduction

WPT system to achieve the power supply and power load without physical contact under the power transmission, with high reliability, good security, low maintenance costs and environmental affinity and so on. System have broad application prospects under special conditions such as electric vehicles, wearable electronic equipment, biomedicine and underwater environment [1–2]. Due to the large leakage inductance of the loosely coupled transformer, in order to reduce the reactive power in the system and reduce the switching loss and the capacity of the power supply, reactive compensation circuit should be added in the primary and secondary. The traditional compensation methods mainly include series compensation and parallel compensation. Four kinds of compensation methods can be obtained by performing series or parallel compensation separately in the primary and the secondary. Reference [3] analyzes the four basic compensation modes from the impedance characteristic, the frequency characteristic and the output characteristic three aspects

[1]School of Economics and Management, North China Electric Power University, Beijing 102206, China

[2]Corresponding Author, e-mail: 1717004702@qq.com

has carried on the detailed analysis respectively, finally has drawn the conclusion that four kinds of basic compensation methods are suitable for different applications respectively. The parallel resonant frequency of resonant compensation is related to the load resistance. Therefore, Compensation is not suitable for secondary compensation of variable load or multi-load WPT systems. In order to meet different requirements, some new compensation topologies have been put forward at home and abroad. Among them, the research of LCL-S WPT system is more prominent. Due to its stable operating frequency of the system resonance, constant primary coil current and constant system output voltage, it can be used in large scale applications such as electric vehicle charging and desktop multi-load power supply [4–5].

Figure 1 shows the equivalent circuit model of the LCL-S WPT system, where Ud is the DC voltage source, S1 to S4 are IGBTs and D1 to D4 are their anti-parallel diodes respectively. Lp and LS are respectively the primary and secondary windings Inductance, M mutual inductance; L1 is the primary compensation inductance, C1 is the primary compensation capacitor; C2 is the secondary compensation capacitor; Uin, Iinare the inverter output voltage and current; Ip, Is respectively the primary Coil current, secondary coil current; R is the system equivalent resistance load; Uo, Io respectively the system output voltage and current. The working frequency of the system is f, among them, f0 is the systematic resonance working frequency.

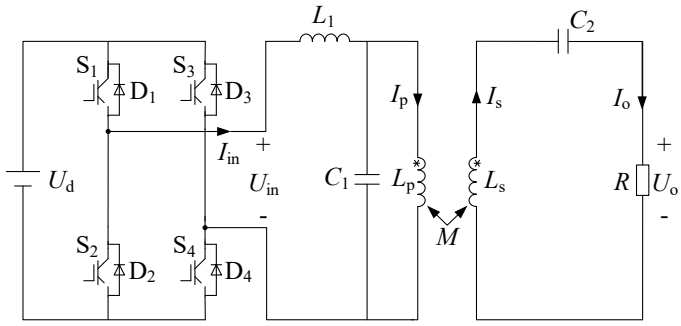

Fig. 1. Equivalent circuit model of LCL-S WPT system

Through theoretical analysis, when the system parameters in Figure 1 satisfy the relation of (1)

$$\begin{cases} \omega_0 = 2\pi f_0 \,, \\ \omega_0 = 1/\sqrt{L_p C_1} \,, \\ \omega_0 = 1/\sqrt{L_s C_2} \,, \\ L_1 = L_p \,. \end{cases} \tag{1}$$

The primary winding current I_p, the system output voltage U_o and the inverter output system total impedance Z_{in} can be calculated as follows:

$$I_p = \frac{U_{in}}{\omega_0 L_1} \,, \tag{2}$$

$$U_o = \frac{M U_{in}}{L_1} \,, \tag{3}$$

$$Z_{in} = \frac{L_1^2 R}{M^2}\,. \tag{4}$$

It can be seen from Eq. (2) and Eq. (3) that the primary coil current I_p and the system output voltage U_o are independent of the system equivalent resistance, indicating that the system has the primary coil constant current characteristics and the system Output voltage constant characteristics, can be more than one electric vehicle constant voltage charging. At the same time, it can be seen from Eq. (4) that the total impedance Z_{in} of the inverter output system always shows a pure resistivity. That is, the change of system equivalent resistive load R does not affect the natural resonant frequency of the system.

The previous analysis is based on the fundamental components of the inverter output voltage U_{in}, and does not consider the harmonic components of the inverter output voltage. The traditional LCL-S type WPT system adopts the voltage type full-bridge inverter circuit. Under the condition that the drive circuit is controlled by the 180 ° conduction mode, the expression of the inverter output voltage u_{in} is

$$u_{in} = \frac{4U_d}{\pi}\left(\sin\omega t + \frac{1}{3}\sin 3\omega t + \frac{1}{5}\sin 5\omega t + \cdots\right). \tag{5}$$

among them, $\omega = 2\pi f$.

In order to analyze the influence of the harmonic component of the inverter output voltage on the LCL-S type WPT, taking the 3rd and 5th harmonic voltage as an example, the specific analysis will be carried out as follows.

In the fundamental voltage under the secondary impedance Z_{21} system

$$Z_{21} = j\omega L_s + j\omega C_2 + R\,. \tag{6}$$

Its total reflection to the primary side of the system is Z_{r1}

$$Z_{r1} = \frac{(\omega M)^2}{Z_{21}} = \frac{(\omega M)^2}{j\omega L_s + j\omega C_2 + R}\,. \tag{7}$$

After the inverter output level system total impedance $Z_{in1:}$

$$Z_{in1} = j\omega L_1 + \frac{1}{j\omega C_1 + \dfrac{1}{j\omega L_p + Z_{r1}}}\,. \tag{8}$$

Fundamental component I_{in1} of inverter output current i_{in} is:

$$I_{in1} = \frac{\dfrac{4U_d}{\sqrt{2}\pi}}{Z_{in1}} = \frac{\dfrac{4U_d}{\sqrt{2}\pi}}{j\omega L_1 + \dfrac{1}{j\omega C_1 + \dfrac{1}{j\omega L_p + Z_{r1}}}}\,. \tag{9}$$

Similarly, the third harmonic component and the fifth harmonic component of

the inverter output current i_{in} can be obtained as

$$I_{in3} = \frac{\dfrac{4U_d}{3\sqrt{2}\pi}}{j3\omega L_1 + \dfrac{1}{j3\omega C_1 + \dfrac{1}{j3\omega L_p + Z_{r3}}}}, \tag{10}$$

$$I_{in5} = \frac{\dfrac{4U_d}{5\sqrt{2}\pi}}{j5\omega L_1 + \dfrac{1}{j5\omega C_1 + \dfrac{1}{j5\omega L_p + Z_{r5}}}}, \tag{11}$$

$$Z_{r3} = \frac{(3\omega M)^2}{j3\omega L_s + j3\omega C_2 + R}, \tag{12}$$

$$Z_{r5} = \frac{(5\omega M)^2}{j5\omega L_s + j5\omega C_2 + R}. \tag{13}$$

This can be obtained from the inverter output current harmonic distortion rate $THD_{i_{in}}$

$$THD_{i_{in}} = \frac{\sqrt{(I_{in3})^2 + (I_{in5})^2}}{I_{in1}}. \tag{14}$$

The formula (14) can be drawn on the inverter output current harmonic distortion $THD_{i_{in}}$ and load R two-dimensional relationship, shown in Figure 2.

As can be seen from Figure 2, when the load R is large, the inverter output current harmonic distortion rate is larger, which will lead to larger inverter losses, lower system efficiency, but also exacerbated the system instability. Aiming at this problem existed in the light load of the original system, two improved methods are proposed in this paper, which will be described separately.

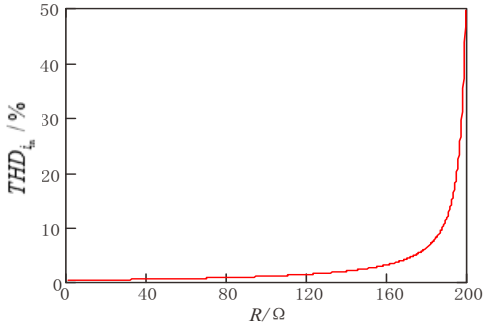

Fig. 2. Relationship between harmonic distortion of inverter output current and load R of LCL-S WPT system

2. Theoretical analysis of improved LCL-S wireless charging system

In the branch where the original system L_1 is added LC series resonant filter, the improved system circuit shown in Figure 3.

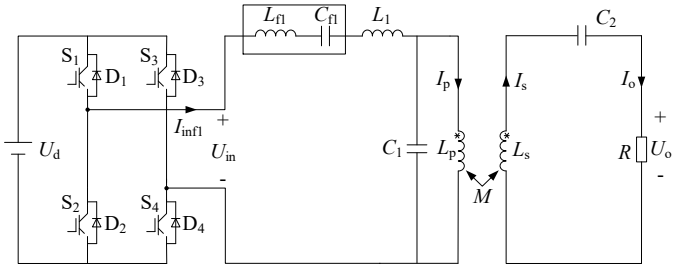

Fig. 3. Equivalent circuit model of A type improved LCL-S WPT system

Among them, L_{f1} and C_{f1} satisfy the following relationship:

$$\omega_0 = \frac{1}{\sqrt{L_{f1}C_{f1}}}. \tag{15}$$

At this moment, only when fundamental components u_{in} be taken into account, the total system impedance $Z_{\text{inf}\,11}$ at the output of the inverter is

$$Z_{\text{inf}\,11} = j\omega L_{f1} + \frac{1}{j\omega C_{f1}} + j\omega L_1 + \frac{1}{j\omega C_1 + \dfrac{1}{j\omega L_p + Z_{r1}}}. \tag{16}$$

Among them, Z_{r1} is the formula (7).

The fundamental component $i_{\text{inf}\,1}$ of the inverter output current $I_{\text{inf}\,11}$ is

$$I_{\text{inf}\,11} = \frac{\dfrac{4U_d}{\sqrt{2}\pi}}{j\omega L_{f1} + \dfrac{1}{j\omega C_{f1}} + j\omega L_1 + \dfrac{1}{j\omega C_1 + \dfrac{1}{j\omega L_p + Z_{r1}}}}. \tag{17}$$

Similarly, the third harmonic component and the fifth harmonic component of the inverter output current $i_{\text{inf}\,1}$ can be respectively

$$I_{\text{inf}\,13} = \frac{\dfrac{4U_d}{3\sqrt{2}\pi}}{j3\omega L_{f1} + \dfrac{1}{j3\omega C_{f1}} + j3\omega L_1 + \dfrac{1}{j3\omega C_1 + \dfrac{1}{j3\omega L_p + Z_{r3}}}}, \tag{18}$$

$$I_{\inf 15} = \frac{\dfrac{4U_d}{5\sqrt{2}\pi}}{j5\omega L_{f1} + \dfrac{1}{j5\omega C_{f1}} + j5\omega L_1 + \dfrac{1}{j5\omega C_1 + \dfrac{1}{j5\omega L_p + Z_{r5}}}}. \tag{19}$$

Among them, Z_{r3} and Z_{r5} are represented by the formulas (12) and (13), respectively.

This can be obtained A type improved LCL-S wireless charging system inverter output current $i_{\inf 1}$ harmonic distortion rate $THD_{i_{\inf 1}}$:

$$THD_{i_{\inf 1}} = \frac{\sqrt{(I_{\inf 13})^2 + (I_{\inf 15})^2}}{I_{\inf 11}}. \tag{20}$$

Contrast system to improve the output current before the inverter harmonic distortion rate $THD_{i_{in}}$ and type A improved inverter output current harmonic distortion rate $THD_{i_{\inf 1}}$ with the load R trend, as shown in Figure 4.

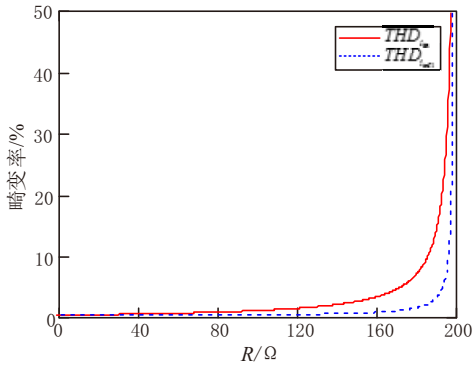

Fig. 4. Comparison of harmonic distortion for inverter output current between A type improved system and original system

It can be seen from Fig. 4, when the load R is large, the harmonic distortion rate of the inverter output current of the A-type improvement system at the light load of the system is obviously decreased compared with that before the improvement, indicating that the A-type improvement system has achieved better performance

3. System simulation and experiment

In order to verify the correctness of the theoretical analysis above, this paper identified the simulation parameters as list in Table 1.

Table 1. Simulation and experimental parameters

parameter	numerical	parameter	numerical
U_d	160/V	C_1	0.15/ μ F
f_0	20/kHz	C_2	0.15/ μ F
L_p	105/ μ H	L_{f1}	158/ μ H
L_s	105/ μ H	C_{f1}	0.1/ μ F
M	21/ μ H	L_{f2}	158/ μ H
L_1	105/ μ H	C_{f2}	0.1/ μ F

3.1. Simulation analysis

According to the parameters in Table 1 and Figure 1 and Figure 3, corresponding simulation models were built based on MATLAB/SIMULINK.

When the load resistance R is chosen as 190 Ω, the inverter output current of the original system, improvement system are shown in Figure 7(a), Figure 7(b) respectively.

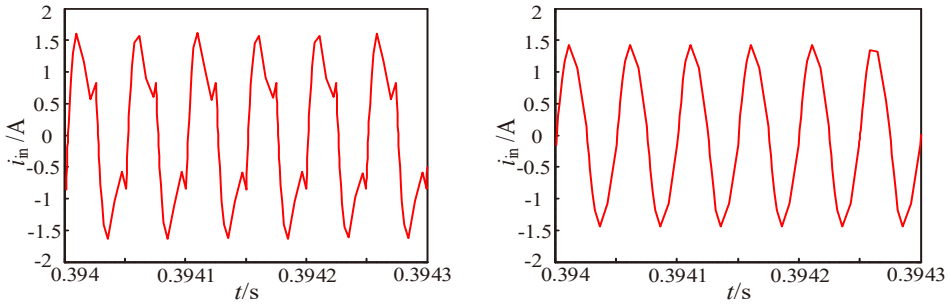

(a) original system (b) improvement system

Fig. 5. Simulation waveforms of inverter output current for different systems

It can be seen from Figure 7 that the inverter output current waveforms of the improvement system smoother than the original system inverter output current waveforms. It can be seen intuitively that the improved systems have achieved good results. Wherein, the improved system achieved the best improving effect.

All the waveforms in Figure 7 were Fourier analysis of the harmonic histogram shown in Figure 8.

As can be seen in Figure 8, compared with the original system, the total harmonic distortion rate of the improved systems decreased by 82.37 % and 55.03% respectively. As can be seen from the data, the improved systems can achieve better results.

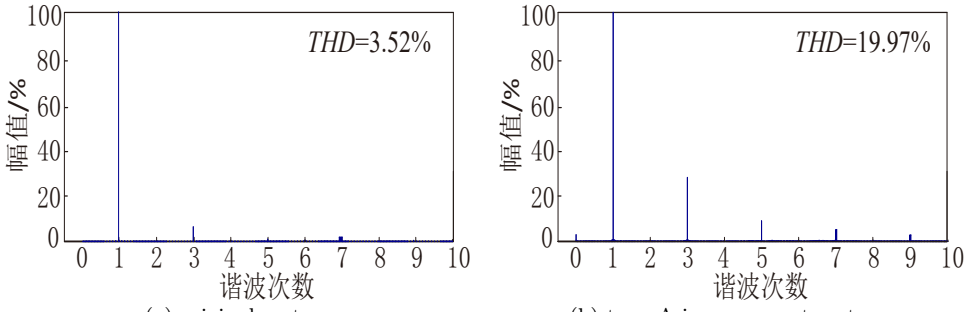

(a) original system (b) type A improvement system

Fig. 6. Inverter output current harmonic histogram of different system

3.2. Experimental Analysis

According to the experimental parameters in Table 1 and Figure 1, Figure 3, corresponding experiment platform were set up, respectively.

When the load resistance is chosen to be 190 Ω, the inverter output current waveforms of the original system and the improvement system are shown in Figs. 9(a) and 9(b), respectively.

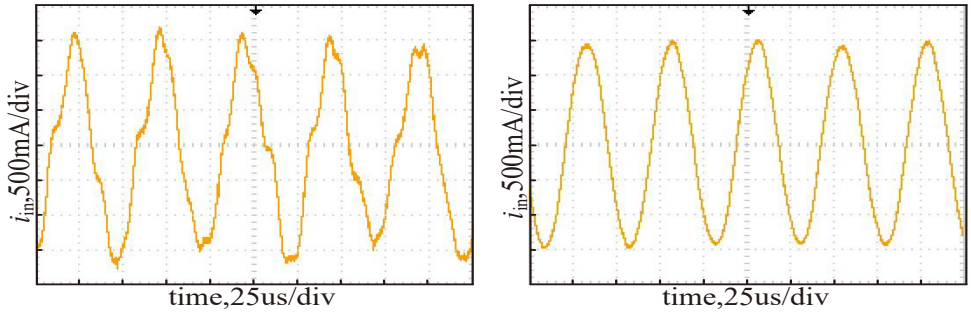

(a) original system (b) improvement system

Fig. 7. Experimental waveforms of inverter output current for different systems

It can be seen from Fig. 9 that the experimental waveforms of the inverter output current of the improved systems smoother than that of the original system inverter output current test waveforms, which is in good agreement with the previous theoretical analysis and simulation analysis.

4. Conclusion

This paper analyzed the inverter output current distortion problem that exists in the traditional LCL-S WPT system when system is light loaded. The root cause of this problem is pointed out. And two improved methods are proposed, which have been proved to be effective and feasible from three aspects: theoretical analysis,

simulation and experimental verification. Both of the improved methods can well solve the problems existing in the traditional LCL-S WPT system, and can achieve good results for improving the inverter output current waveform and reducing the inverter switching loss so as to improve the system efficiency. It will be of great benefit to its application in a wireless charging system for electric vehicles.

References

[1] Xun L., S. Y. Hui.: *Optimal Design of a Hybrid Winding Structure for Planar Contactless Battery Charging Platform.* IEEE Transactions on Power Electronics *23* (2008), No. 1, 455–463.

[2] Cao Lingling, Chen Qianhong, Ren Xiaoyong, et al. : *Review of the efficient wireless power transmission technique for electric vehicles.* Transactions of China Electrotechnical Society *27* (2012), No. 8, 1–13.

[3] MA Hao, SUN Xuan.: *Design of Voltage Source Inductively Coupled Power Transfer System with Series Compensation on both sides of transformer.* Proceedings of the CSEE *30* (2010), No. 15, 48–52.

[4] Zhang Hui, Wang Huimin, Li Ning, et al. : *Analysis on Hybrid Compensation Topology Circuit for Wireless Charging of Electric Vehicles.* Automation of Electric Power Systems *40* (2016), No. 16, 71–75

[5] Tang Xiaowen, Yao Gang, Yao Changzheng, et al.: *The contactless power transfer system based on LCL compensation.* Power Electronics *49* (2015), No. 10, 7–10.

Received November 16, 2017